Chemical Physics Letters 644 (2016) 45–50

Contents lists available at ScienceDirect

Chemical Physics Letters

journal homepage: www.elsevier.com/locate/cplett

Bayesian separation algorithm of THz spectral sources applied to D-glucose monohydrate dehydration kinetics

L.A. Sterczewski*, M.P. Grzelczak, K. Nowak, B. Szlachetko, E.F. Plinski

Wroclaw University of Technology, Department of Electronics, 27 Wybrzeze Wyspianskiego St., Wroclaw 50-370, Poland

ARTICLE INFO

Article history:
Received 30 July 2015
In final form 19 November 2015
Available online 26 November 2015

ABSTRACT

An estimation of the dehydration kinetics of monohydrated D-glucose with the use of the Bayesian spectral source separation algorithm is described. The dehydration experiment was probed with the terahertz time domain spectroscopy (THz-TDS). Contrary to the widely used peak-area method, our approach to the quantitative analysis takes into account the full spectral information. The obtained concentration profiles at different temperatures were processed in order to measure the kinetics of the dehydration process. Our investigation shows that the proposed method may be used to estimate the evolution of concentration despite the overlapping peaks and multiple spectral sources in the observed spectra.

1. Introduction

When observed signals are mixtures of pure spectra mixed in unknown proportions and evolving in time, a blind source separation problem (BSS) can be considered [1]. There is a special class of signal processing algorithms, which allow an estimation of pure spectral components and the corresponding mixing coefficients. Under the assumption of statistical independence, a well-known independent component analysis (ICA) [2] is capable of unmixing spectral mixtures. However, the problem is still difficult due to the constraints of the non-negative absorbance and the full additivity (sum-to-one) of the mixing coefficients. The algorithm of the hierarchical Bayesian separation of spectral sources, which meets the above requirements, was proposed in 2006. This algorithm is an enhancement of the blind source separation class of algorithms [3]. The effectiveness of the statistical methods has already been confirmed in [4,5]. In particular, the Hierarchical Bayesian BSS is an efficient way to resolve the concentration profile and pure spectral components of the chemical compounds with strongly overlapping absorption peaks. Alternatively, reports on the application of the principal component analysis (PCA) to the analysis of the multicompound spectral mixtures in phase transitions can also be found in the literature [6,7]. However, the representation of data points yielded by the PCA in the new coordinate system, makes the estimation of the concentration evolution non-trivial.

Spectroscopic studies of solids with the use of the terahertz time-domain spectroscopy, carried out in the spectral region between 0.3 and 3 THz (10 and 100 cm^{-1}), enabled a characterization of pharmaceuticals and their polymorphic transitions [8–10]. The dehydration process is one of the pseudo-polymorphic transitions, which can be probed and characterized with the THz-TDS technique.

In this letter we report the successful application of the hierarchical Bayesian blind source separation algorithm for quantity evaluation of pure spectral components of the evolving spectra. We studied the dehydration rate of a polycrystalline hydrate – the D-glucose monohydrate in the terahertz regime. The results of the BSS algorithm-based quantity estimation of the dehydrate are compared with peak-area method used previously [11].

The Bayesian spectral source separation algorithm generates the unmixed spectra by means of iterative sampling from the multidimensional probability density functions with the carefully selected prior distributions. The Gamma, Dirchlet and normal distributions are assumed for the spectra, concentrations and noise, respectively. Full implementation details, and the underlying samples' drawing technique can be found in the literature [4]. The working principle of the algorithm is to find such statistically independent spectra, that mixed together create the observations. It is also required that pure spectral sources to be estimated do not have Gaussian distributions. In the harnessed algorithm spectra and mixing coefficients α_i are modeled by the Gamma distribution with a shape parameter α and a scale parameter β to be estimated. That distribution is a member of the exponential family and, in particular cases, it becomes the Rayleigh, the chi-squared, and, obviously, the exponential distribution, covering a wide range of spectral shapes [3].

* Corresponding author.
E-mail address: lukasz.sterczewski@pwr.edu.pl (L.A. Sterczewski).

http://dx.doi.org/10.1016/j.cplett.2015.11.031
0009-2614/

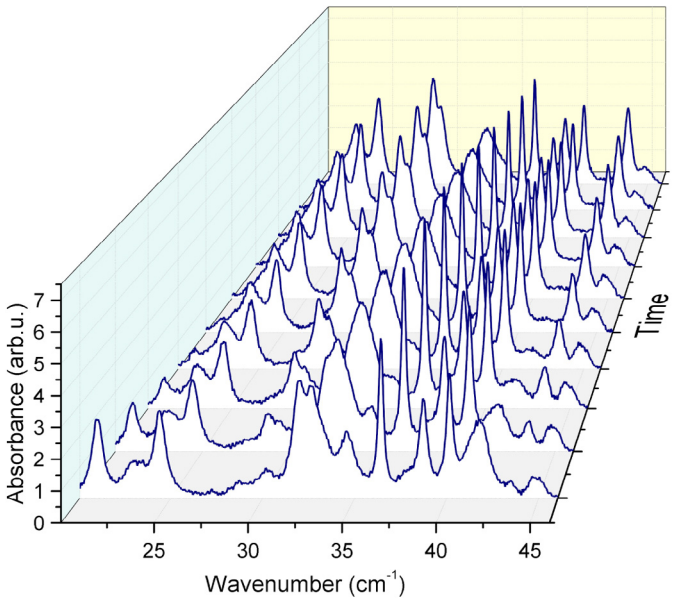

Figure 1. Evolving-in-time mixture of three synthetic spectra with Gaussian and Lorentzian absorption peaks shapes. Positions of the peaks in pure spectral components, to be estimated, were random.

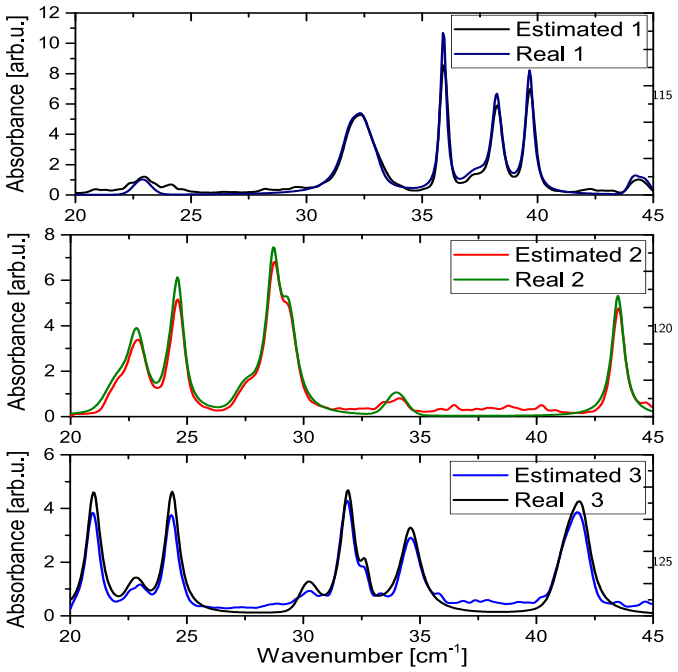

Figure 2. Estimated pure spectra obtained in the synthetic experiment.

This assumption can be empirically verified by calculating a histogram of a single-component spectrum, which, simply speaking, is an estimate of the continuous probability density function (distribution). The histogram of the pure spectral component should converge to the Gamma distribution function depending on the number or spectral bands and histogram bins.

When the spectra are linearly mixed, the distribution function of their linear sum is no longer Gamma. According to the Central Limit Theorem, a sum of independent random variables follows approximately the Gaussian distribution, at least is more Gaussian, than the any of the pure components. That difference in the distribution function enables us to resolve the mixed spectra and the evolving in time mixing coefficients to estimate the kinetics, as the algorithm finds for the most non-Gaussian statistically independent spectra possible.

2. Proof of concept for algorithm

In order to demonstrate that the BSS algorithm can accurately estimate the concentration, three synthetic spectral sources were generated with randomly distributed Gaussian and Lorentzian-shaped absorption peaks (but spectra were not normally distributed).

The evolving-in-time mixing coefficients followed the exponential and gamma curves as such curves are often met in e.g. phase transitions. The full additivity constraint, equivalent to the sum-of-one of the mixing coefficients, was also respected at each time instant. Figure 1 shows the resulting spectral mixtures. These mixtures have been resolved without any prior knowledge of either the concentration evolution or the shape of the spectra (except for the probability density function). The procedure is depicted in Figures 2 and 3. The overlapping peaks in the 20–27 cm^{-1} and the 30–35 cm^{-1} regions have not disturbed the quality of the estimates.

In the first step, the virtual experiment has shown that the constrained BSS algorithm can be a valuable tool for the quantitative analysis of multiple-compound spectral mixtures with strongly overlapping peaks. In the next step, the algorithm was applied to the dehydration process analysis of the aforementioned α-D-glucose monohydrate.

3. Experimental

The D-(+)-glucose monohydrate, purchased from Sigma–Aldrich, was ground in a mortar into fine particles and diluted with 360 mg of low grade polyethylene powder from TeraView (UK). The resulting 400 mg of powder (40 mg of D-(+)-glucose) was compressed into a 3 mm thick pellet with a diameter of 13 mm by using a hydraulic press (the pressure applied was 2 tons for 2 min). The thickness of the samples was chosen to match the previous studies on polyethylene pellets in the terahertz spectroscopic experiments so as to avoid the etalon effect and the saturation of absorption [12].

The beam of the 780 nm femtosecond laser (82 fs, 100 MHz, Menlo Systems) was split by a 50:50 non-polarizing beam splitter into two beams of 10 mW. These two beams pumped and probed the low-temperature grown gallium arsenide photoconductive antennas (LT-GaAs PCA). To increase the signal-to-noise ratio, the transmitting antenna was biased with a 20 kHz 30 V

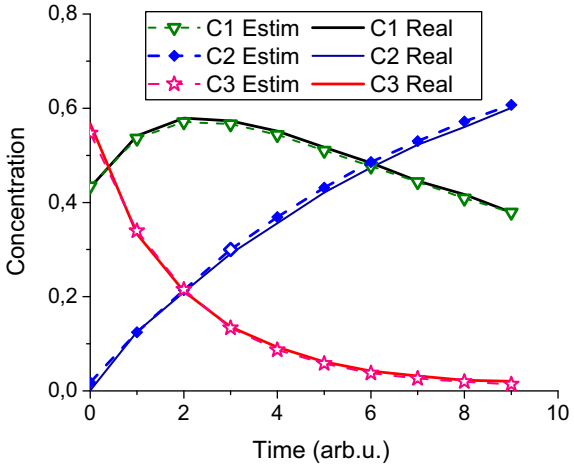

Figure 3. Estimated evolution of the concentration profile obtained in the synthetic experiment, which shows good level of match with the real values.

bipolar square wave chopping signal, instead of a mechanical chopper [13]. The generated THz pulses were guided, collimated and focused by four off-axis parabolic mirrors. A custom-made sample heater was placed in the focal point of the optical system. The terahertz pulses were propagated in a dry nitrogen atmosphere, to minimize the effect of water vapor THz absorption lines in ambient air. The terahertz electric field was detected by the receiving photoconductive antenna connected to the lock-in amplifier, synchronized with the chopping signal. The time shift of the probing laser pulse was introduced by the mechanical stage. We measured the transmission through a 360 mg reference polyethylene pellet and the monohydrous glucose pellets. Samples were held at the constant temperature for 240 min at 40 °C, 180 min at 42 °C, and 80 min at: 44 °C, 46 °C, 48 °C, and 50 °C to measure the dehydration process. It took approximately 150 s for each waveform to be acquired. 50 terahertz signals were accumulated and averaged enhancing the dynamic range (>60 dB).

The 20 ps long time-domain signals were four times zero-padded. Next, by applying the Fourier transform, the spectra were calculated with a spectral resolution of 50 GHz. The absorption spectra were calculated using the standard mathematical procedure [14,15]. This method allows diminishing the spectral effects of the diluent and the spectrometer. To compensate the effect of a varying with wavenumber baseline, we harnessed a top-hat operation filtering algorithm. One of well-established methods of the baseline removal is fitting a polynomial. Its major drawback is that it boosts slight variations from the smooth polynomial curve, thus the fitting procedure requires a careful choice of the model order and the fitting region (alternatively the support points). For best results, each spectrum should be fitted individually with the baseline curve but such procedure introduces many degrees of freedom in spectra preprocessing. Not only is it computationally ineffective but also it requires a researcher interaction.

An alternative approach involves morphological operations, which have found application in image processing to enhance contrast between small elements and details surrounded by a large and non-smooth background. In a one-dimensional case, morphological operations were successfully applied in mass-spectrometry data to eliminate a slowly-varying baseline without prior knowledge about the complex baseline shape [16]. A representative of the morphological filter class – the top hat operator ($\hat{\circ}$) – subtracts from the source spectrum I its morphological opening ($\circ$).

$$I\hat{\circ}S = I - I \circ S = I - ((I \ominus S) \oplus S), \tag{1}$$

where $\ominus$ and $\oplus$ denote erosion and dilation operation, respectively. The top-hat operation removes from the spectrum elements larger than the structuring element S. The peak extraction procedure can be divided into two steps. Firstly, the erosion operator $\ominus$ searches for the local minimum of the spectrum on a given interval, defined by the size of the structuring element S. This operation trims the absorption peaks narrower than S and shifts the spectrum to higher wavenumbers. Secondly, the dilation operator $\oplus$ performs the search for the local maximum on the 'eroded' spectrum, restoring the initial position of the elements on the wavenumber axis. A product of this two-step operation – the morphological opening – is the unwanted background without the extracted peaks. Its subtraction from the input spectrum leaves the sharp peaks only. This peak extraction technique has been recently proposed in application to the terahertz time-domain spectroscopy [17].

As the baseline shape in spectroscopic data is not constant, it is non-trivial to determine the actual depth of the absorption peaks. Intuitively, the size of the structuring element S should be slightly larger than the width of the peaks but much smaller than wide background elements. Favorably, it is the only one variable parameter in the top-hat morphological baseline removal, identical for all processed spectra. In contrast to the polynomial fitting procedure, it is an effective and fast procedure, easy to parallel for large throughput data, like in the case of the phase transition experiments. The shape of the top-hat-processed spectrum does not strongly depend on the choice of the spectral window considered.

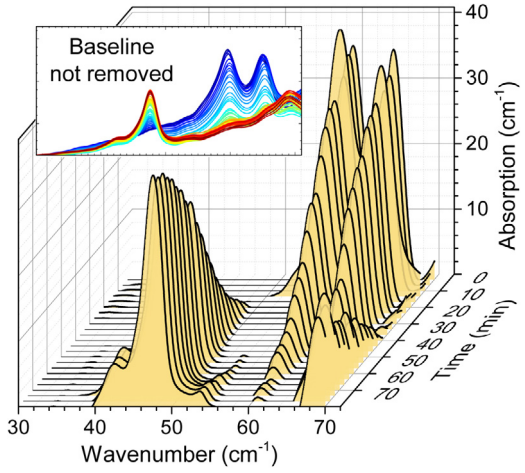

Figure 4. Spectral evolution of glucose heated at 46 °C with corrected baseline by the top-hat filtering algorithm (size of the structuring element was 20 cm^{-1}). The inset shows the raw uncorrected spectrum.

An undisputed fact, favoring the top-hat filter over the polynomial fitting for the blind source separation procedure, is that it makes the input spectra sparse. The regions, where no spectral peaks are present, are efficiently zeroed. As a result, the spectra are said to be zero-grounded, that is, with a large number of entries close to zero. The corresponding distribution function for the sparse spectrum will follow the exponential-like function, which is less Gaussian than a typical Gamma curve. The quality of the estimates, considering the constraints for the probability distribution in the blind source separation, will be considerably better. The peak-area method also requires a reliable technique to extract the absorption peaks, which are further integrated, thus we decided to employ this novel method in terahertz spectroscopic studies.

Since the choice of the aforementioned structuring element may affect the estimates of the concentration, in our experiment we considered its three different sizes: 10 cm^{-1}, 20 cm^{-1}, and 30 cm^{-1}, corresponding to the width of the dehydrated glucose peak, hydrated glucose peaks, and the 'fingerprint' phase transition spectral region.

The evaluation of the fraction of the dehydrated D-glucose (α) was performed with the use of two methods, which we later compared. Referring to [11] we integrated the absorption peak area between 39.7 cm^{-1} (1.19 THz) and 52.0 cm^{-1} (1.56 THz) of the normalized spectra. *Per contra* we harnessed the BSS algorithm to estimate the quantity of the dehydrated D-glucose from the spectra evolving in time in the 20–80 cm^{-1} range (0.6–2.4 THz). The second approach used the full-band spectral information. Figure 4 shows the evolution of the THz absorption spectrum of D-glucose at 46 °C. The inset illustrates the motivation for baseline removal – the evolving spectra are non zero-grounded, what is essential for the two α coefficients estimation methods.

4. Results and discussion

It was previously shown (2006), that the dehydration of D-glucose monohydrate in a polyethylene pellet can be modeled, with a good level of match, by the two-dimensional contracting area equation (R2) [11,18]

$$1 - (1 - \alpha)^{1/2} = kt, \tag{2}$$

Table 1
The correlation coefficient, sum of RSS, and activation energy obtained with different numerical procedures.

α-Eval. method	Filter size $\lvert S\rvert$ [cm^{-1}]	Correlation coefficient r of Eq. (7)	Sum of RSS ($\sum$RSS)	Activation energy E_A [$kJ\,mol^{-1}$]
PA-R1	10	−0.9702	0.2337	154.8
PA-R2	10	−0.9680	0.2966	170.6
PA-R1	20/30	−0.9595	0.3319	146.1
PA-R2	20/30	−0.9500	0.4527	158.6
BSS-R1	10	−0.9818	0.2299	131.6
BSS-R2	10	−0.9784	0.2604	144.5
BSS-R1	20	−0.9870	0.3259	129.7
BSS-R2	20	−0.9810	0.3357	140.0
BSS-R1	30	−0.9870	0.3493	129.5
BSS-R2	30	−0.9820	0.3544	139.4

where α is the normalized fraction of the dehydrate, k is the dehydration rate constant, and t is time. In a more recent work (2011), authors have encountered a problem, that the choice of the underlying rate law is mostly based on correlation coefficients of the fit to the (α, t) data, and even small perturbations in the α evaluation can result in best fitting with different models [19]. They proposed a new model for the dehydration of α-D-glucose – a one dimensional contraction rate law (R1).

$$1-(1-\alpha)^{2/3}=kt. \tag{3}$$

The dehydration of glucose monohydrate in their experiment was studied using isothermal gravimetric analysis in the temperature range 59.8–80.2 °C.

For the two α estimation methods we compared three baseline removal scenarios and two kinetic models from the above equations. The results are summarized in Table 1. The α evaluation methods are divided into two groups, as introduced earlier: the peak-area (PA), and the blind source separation (BSS). The element following a dash determines the dehydration model used: the 1D or 2D contracting rate law, R1 and R2 respectively. The high correlation coefficients of the linear fits to the dehydration model (>0.90) were obtained for both methods and models of the dehydrate fraction estimation (not shown). However, the linear fits to the contraction rate model yielded by the BSS method were slightly better. Seeing that the correlation coefficient may not be sufficient to compare the performance of the α evaluation methods, the residual sum of squares (RSS) was used, which measures the difference between the measurement-based estimates and the ideal model

$$RSS(j)=\sum_{i=1}^{n}(1-(1-\alpha_{ij}))^{1/m}-(\hat{a}+kt_i))^2, \tag{4}$$

where k is the estimated dehydration rate constant (slope), $\hat{a}$ is the estimated constant term, m is the dehydration model constant (n=2 for R2, n=1.5 for R1) and α_{ij} are the normalized dehydration fractions estimated by one of the methods extracted from the spectrum at the ith time instant and the jth temperature point. To take into account the fits at different temperature points j and describe them with a single numerical quantity, a sum of RSS measures the quality of the dehydration model and the baseline removal method

$$\sum RSS=\sum_{j=1}^{6}RSS(j). \tag{5}$$

Comparing the sum of RSS from Table 1, it can be seen that the updated rate law (R1) fits better the experimental data than the previously proposed model (R2), when the same baseline removal technique is used. Additionally, one can conclude the optimal filter size $\lvert S\rvert$. Generally, the 10 cm^{-1} filter, slightly wider than the peak to extract, but not too wide, resulted in the lower value of the sum of RSS, indicating a better model fit for the two α coefficient estimation methods. The peak area method (PA-Rn) did not distinguish between the spectra processed with the 20 cm^{-1}, and 30 cm^{-1} wide filter, as the estimates were the same. In the case of the BSS method a difference between the 20 cm^{-1}, and 30 cm^{-1} filter size is insignificant. Figure 5a and b shows the dehydration kinetics according to the one-dimensional contraction rate law (R1) from Eq. (2), estimated using the BSS algorithm and the aforementioned peak-area method for the lowest ΣRSS case.

The dehydration rates k – the slopes of the kinetic law fits – were used to generate the Arrhenius plot which relates ln k to $1/T$ (Figure 6a and b). The Arrhenius reaction rate equation is given by

$$k(T)=A\exp(-E_A/RT), \tag{6}$$

where A is the pre-exponential constant factor, E_A is the activation energy ($kJ\,mol^{-1}$), R is the universal gas constant ($8.314\cdot10^{-3}\,kJ\,mol^{-1}\,K^{-1}$), and T is the absolute temperature in Kelvin. By taking the logarithm of both sides, Eq. (6) can be rewritten in the Arrhenius plot-ready form

$$\ln(k(T))=\frac{-E_A}{R}\frac{1}{T}+\ln(A). \tag{7}$$

This equation gives the linear relationship between $\ln(k)$ and $1/T$ with an intercept $\ln(A)$, and a slope E_A/R. By fitting a straight line to the Arrhenius plot generated separately for the BSS and the peak-area method from the dehydration rates k, values of the activation energy were calculated as in the last column of Table 1. The third column includes the corresponding correlation coefficient of the fit to Eq. (7). This procedure yielded ten values of the activation energy of the dehydration, from which the best-fitting experimental data are: 131.6 $kJ\,mol^{-1}$ for the BSS method, and 154.8 $kJ\,mol^{-1}$ for the peak-area method, with the corresponding correlation coefficients of r_{BSS}=−0.9818, and r_{PA}=−0.9702 respectively. In both cases the updated rate law (R1) from Eq.(3) fits better than the previously proposed dehydration model in THz regime (R2). However, the best fit (emphasized with bold font in the table) was obtained with the Bayesian blind source separation method and the 10 cm^{-1} structuring element.

In our experimental conditions the derived activation energy of the D-glucose monohydrate dehydration is slightly different from the literature value for the terahertz time-domain spectroscopic studies (149 $kJ\,mol^{-1}$) [11]. On the other hand, the baseline removal procedure is not described in details, what makes a direct comparison between studies difficult. In the peak-area method with the contracting area equation model (R2) and the non-optimal choice of the structuring element baseline removal method we obtained 158.6 $kJ\,mol^{-1}$ for this parameter. If we consider the goodness of fit regarding the structuring element size, the activation energy, evaluated using the peak area method and the same dehydration law (R2) with the 10 cm^{-1} wide S, is 170.6 $kJ\,mol^{-1}$.

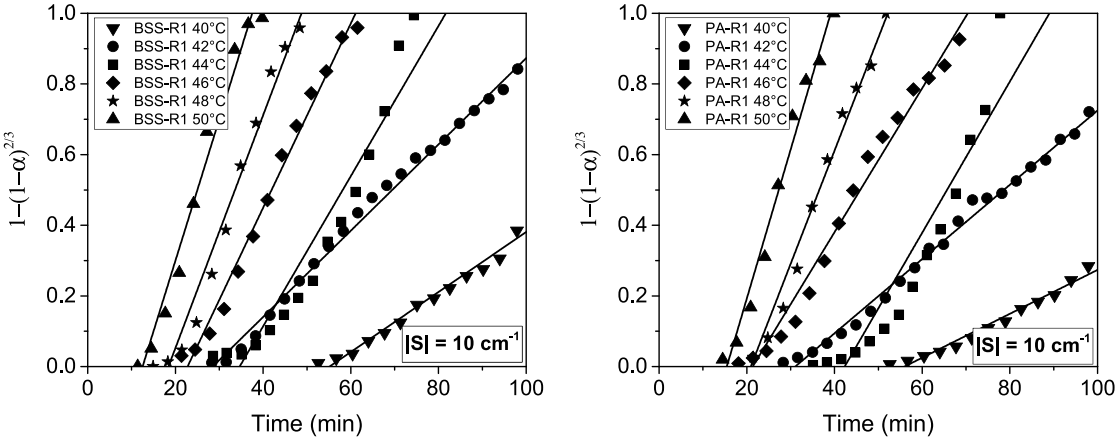

(a) The BSS method (b) The peak-area method

Figure 5. Dehydration of α-D-glucose monohydrate evaluated according to the 1D contraction rate law of the solid-state reaction. Figures illustrate the best fits (high r and the lowest ΣRSS) for the two methods used for estimation of the normalized dehydration fraction α with a reasonable choice of the structuring element size. A slight improvement with the BSS scenario can be seen.

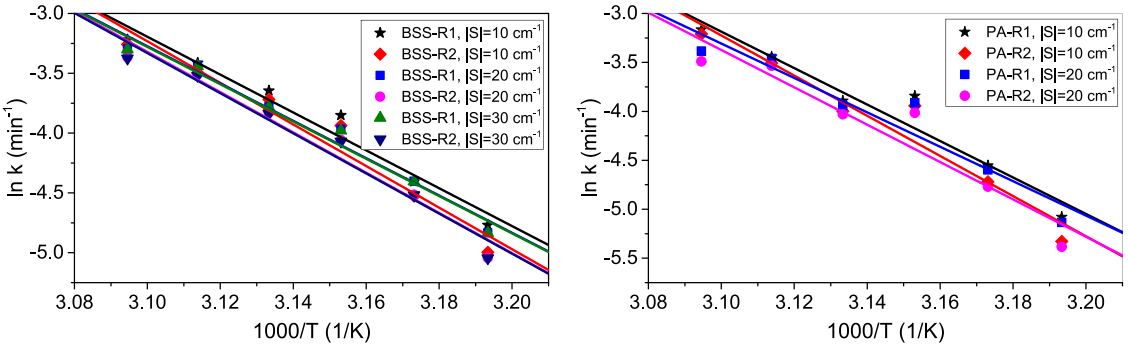

(a) The BSS method (b) The peak-area method

Figure 6. The Arrhenius plot of the α-D-glucose monohydrate dehydration generated with two α evaluation methods. In the peak area method the baseline removal scenarios with the 20 cm^{-1} and 30 cm^{-1} wide structuring element gave identical results.

The obtained activation energy also differs from the literature value for the recently proposed 1D contraction rate law (R1 -65.0 ± 3.9 kJ mol^{-1}) [19]. Authors, however, studied the dehydration using gravimetric analysis in a higher temperature range ($\geq$ 59.8 °C), without the support of spectroscopy. In the same work it was shown that physical parameters of the sample have a strong effect on the extent of lost water during dehydration at a constant temperature with the same heating time. Nonetheless, it appears that in spectroscopic studies of the glucose monohydrate dehydration the calculated activation energy can be twice as high as obtained with the thermal method. For this reason the use of only one technique to monitor the dehydration process may not be sufficient. Recently, monitoring dehydration kinetics using spectral and thermal methods simultaneously has been successfully implemented [20].

This study has shown that the obtained value strongly depends on the estimation method and the underlying dehydration model assumed. The difference between the lowest and highest value of E_A exceeds 40 kJ mol^{-1}, almost 30% of the reference value.

5. Conclusions

Application of the Bayesian spectral source separation algorithm to study the dehydration kinetics was presented. The described method can be a convenient alternative to the widely-used peak-area method of pure component's fraction coefficient estimation in multi-compound spectral mixtures with fully additive spectra. The proof-of-concept performed for the algorithm confirmed that strongly overlapping peaks, even in three-component mixture, did not perturb the estimates. The evolution of the estimated concentration vector in time shows an agreement with that obtained in a synthetic experiment.

For the real data experiment, the Bayesian algorithm based estimates of the concentration vector exhibit higher values of the linear correlation coefficient to the dehydration model and mostly lower sum of RSS, than those based on the peak-area method. Additionally, unlike the other statistical methods, the separation algorithm draws the spectra and concentration profile evolution in an easy-to-process form (e.g. not in the principal components space). Regrettably, the Bayesian method of source separation has one significant drawback. The method can be applied only, when significant changes in the spectra are observed. The lack of these during the observation time leads to unreliable results of the estimates. The spectral unmixing procedure requires simply the diversity of the spectral data. Nevertheless, such results are easily detectable by analyzing the reconstruction error of the spectra described in [4]. Similarly to the peak-area method, the spectra for the BSS must be preprocessed with a baseline-removing algorithm. Otherwise the Gamma distribution model cannot be assumed.

Our result of the activation energy differs from the previously reported one for several reasons. We chose a different thickness of the samples with respect to the studies presented in [11]. Different parameters of the prepared sample and different experimental conditions have an impact on the final value of the empirically-determined parameter. Additionally, the baseline compensation, introduces a degree of freedom in the processing of spectra, which is a general problem in THz spectroscopy. Various methods are used to eliminate the influence of the baseline, thus a direct comparison of spectroscopic results may be impossible. Scattering of the two forms: the hydrate and dehydrate is different in the higher frequency (wavenumber) regions and depends on the thickness of the sample [11]. An increased scattering is observed as an enhancement of the baseline of the dehydrate. For this reason the choice of the baseline removal profile, which usually remains constant throughout the experiment, may disturb significantly the estimates of the dehydration rates, and eventually the activation energy.

Despite that, the hierarchical Bayesian blind source separation algorithm may be considered a valuable technique for the analysis of the dehydration process. The results, however, may not be equivalent to the peak-area-based investigation.

Acknowledgments

We would like to extend our sincere thanks to Dr. Agata Gorniak from Wroclaw Medical University for the preparation of samples. We also thank Prof. Bede Liu from Princeton University for helpful discussion. This work was supported in part by an internal university grant No. S50036/W4K3.

References

[1] P. Comon, C. Jutten, J. Herault, Signal Process. 24 (1) (1991) 11.
[2] Y.B. Monakhova, S.A. Astakhov, A. Kraskov, S.P. Mushtakova, Chemometr. Intell. Lab. Syst. 103 (2) (2010) 108.
[3] S. Moussaoui, D. Brie, A. Mohammad-Djafari, C. Carteret, Signal Process., IEEE Trans. 54 (11) (2006) 4133.
[4] N. Dobigeon, S. Moussaoui, J.-Y. Tourneret, C. Carteret, Signal Process. 89 (12) (2009) 2657.
[5] F.G. Halaka, G.T. Babcock, J.L. Dye, Biophys. J. 48 (2) (1985) 209.
[6] J.A. Zeitler, K. Kogermann, J. Rantanen, T. Rades, P.F. Taday, M. Pepper, J. Aaltonen, C.J. Strachan, Int. J. Pharm. 334 (1) (2007) 78.
[7] J.A. Zeitler, P.F. Taday, K.C. Gordon, M. Pepper, T. Rades, ChemPhysChem 8 (13) (2007) 1924.
[8] C.J. Strachan, T. Rades, D.A. Newnham, K.C. Gordon, M. Pepper, P.F. Taday, Chem. Phys. Lett. 390 (1) (2004) 20.
[9] J.A. Zeitler, D.A. Newnham, P.F. Taday, T.L. Threlfall, R.W. Lancaster, R.W. Berg, C.J. Strachan, M. Pepper, K.C. Gordon, T. Rades, J. Pharm. Sci. 95 (11) (2006) 2486.
[10] T. Korter, R. Balu, M. Campbell, M. Beard, S. Gregurick, E. Heilweil, Chem. Phys. Lett. 418 (1) (2006) 65.
[11] H.-B. Liu, X.-C. Zhang, Chem. Phys. Lett. 429 (1) (2006) 229.
[12] H. Namkung, J. Kim, H. Chung, M.A. Arnold, Anal. Chem. 85 (7) (2013) 3674.
[13] R. Yano, T. Hattori, H. Shinojima, Jpn. J. Appl. Phys. 45 (11R) (2006) 8714.
[14] Y. Chen, H. Liu, Y. Deng, D. Schauki, M.J. Fitch, R. Osiander, C. Dodson, J.B. Spicer, M. Shur, X.-C. Zhang, Chem. Phys. Lett. 400 (4) (2004) 357.
[15] J.A. Zeitler, T. Rades, P. Taday, Pharmaceutical and Security Applications of Terahertz Spectroscopy. THz Spectroscopy: Principles and Applications, CRC Press, Boca Raton, FL, 2007, pp. 299.
[16] A.C. Sauve, T.P. Speed, Normalization, baseline correction and alignment of high-throughput mass spectrometry data, in: Proceedings Gensips, 2004.
[17] H. Stephani, J. Jonuscheit, C. Robine, B. Heise, Automatically detecting peaks in terahertz time-domain spectroscopy, in: Pattern Recognition (ICPR), 2010 20th International Conference on, IEEE, 2010, p. 4468.
[18] J. Sharp, G. Brindley, B.N. Achar, J. Am. Ceram. Soc. 49 (7) (1966) 379.
[19] M.A. Ponschke, J.E. House, Carbohydr. Res. 346 (14) (2011) 2285, http://dx.doi.org/10.1016/j.carres.2011.07.012.
[20] M.A. Beard, O.R. Ghita, J. McCabe, K.E. Evans, J. Raman Spectrosc. 41 (10) (2010) 1283, http://dx.doi.org/10.1002/jrs.2560.